

## ARTICLE

# Inflammatory and Physiological Consequences of Debridement of Fibrous Tissue after Volumetric Muscle Loss Injury

Benjamin T. Corona, Jessica C. Rivera and Sarah M. Greising\*

Volumetric muscle loss (VML) injuries present chronic loss of muscle fibers followed by expansive fibrotic tissue deposition. Regenerative medicine therapies are under development to promote regeneration. However, mitigation of the expansive fibrous tissue is required for integration with the remaining muscle. Using a porcine VML model, delayed debridement of injury fibrosis was performed 3 months post-VML and observed for an additional 4 weeks. A second group underwent the initial VML and was observed for 4 weeks, allowing comparison of initial fibrosis formation and debrided groups. The following salient observations were made: (i) debridement neither exacerbated nor ameliorated strength deficits; (ii) debridement results in recurrent fibrotic tissue deposition of a similar magnitude and composition as acute VML injury; and (iii) similarly upregulated transcriptional fibrotic and transcriptional pathways persist 4 weeks after initial VML or delayed debridement. This highlights the need for future studies to investigate adjunctive antifibrotic treatments for the fibrosed musculature.

*Clin Transl Sci* (2018) 11, 208–217; doi:10.1111/cts.12519; published online on 28 November 2017.

### Study Highlights

#### WHAT IS THE CURRENT KNOWLEDGE ON THE TOPIC?

✓ The pathophysiology of VML injury is not well understood. The ramifications of surgical debridement of chronic VML-injured tissue are not known, but may conceivably worsen already existing strength deficits and reignite an exacerbated inflammatory and fibrotic response that is not conducive to skeletal muscle regeneration.

#### WHAT QUESTION DID THIS STUDY ADDRESS?

✓ What is the effect of surgical debridement of a chronic VML injury on recurrent tissue fibrosis, intermediate immune responses, and existing functional deficits?

#### WHAT THIS STUDY ADDS TO OUR KNOWLEDGE

✓ These findings indicate that delayed debridement of VML-injured muscle promotes an active inflammatory response that apparently drives robust fibrogenesis and may, therefore, challenge regenerative implants.

#### HOW THIS MIGHT CHANGE CLINICAL PHARMACOLOGY OR TRANSLATIONAL SCIENCE

✓ This work provides a broad array of data characterizing the pathophysiology of chronic VML injury both before and after delayed surgical remediation of the wounded tissue bed, a likely necessary step in the delivery of regenerative medicine therapies. These data are pertinent to translation of regenerative medicine therapies for VML injury.

Volumetric muscle loss (VML) injuries are common in orthopedic trauma and lead to progressive pathophysiology.<sup>1,2</sup> This form of muscle injury is not conducive to canonical skeletal muscle regenerative mechanisms that mediate successful muscle fiber regeneration<sup>3</sup> observed with other recoverable forms of muscle injury, such as crush-induced,<sup>4</sup> ischemia reperfusion-induced,<sup>5</sup> eccentric contraction-induced,<sup>6</sup> and thermal-induced<sup>7</sup> injuries. The loss of key regenerative elements within the VML defect (e.g., satellite cells, fibro-adipogenic progenitors, and the basal lamina) initially limits muscle fiber regeneration. Thereafter, the immune response within the VML defect and surrounding musculature remains heightened and of a mixed pro-inflammatory and anti-inflammatory phenotype,<sup>8,9</sup> which

effectively inhibits myogenic while activating fibrogenic transcriptional pathways. Ultimately, extensive fibrotic tissue deposition envelops the affected muscle compartment,<sup>10</sup> which together with the loss of muscle fibers contributes to limb dysfunction and disability.<sup>11</sup>

The typical course of care for open orthopedic injuries presenting VML, such as type IIIB open fracture, involves provisional stabilization, single or serial wound debridement, definitive stabilization, and soft tissue coverage of the fracture. At this early stage in a presumptive contaminated wound, the highly pro-inflammatory tissue milieu<sup>12</sup> is likely too challenging for currently envisioned regenerative medicine therapies to be successful. Delayed surgical scar revision is a reconstructive option which may,

at best, permit an improvement in motion. Regenerative implantable biological therapies and devices are under development to restore lost muscle tissue and strength. To date, the average time to treatment of VML injury with a regenerative medicine device is 52 months (range, 7–120 months) across 14 patients.<sup>13,14</sup> That being said, the surgical approach in these settings included a thorough surgical debridement to establish connectivity of the regenerative medicine implant with viable muscle tissue, an approach likely to encourage a currently undefined secondary inflammatory response that may induce recurrent fibrosis.

The current work was performed to establish a working knowledge of the effect of surgical debridement of a chronic VML injury wound on recurrent tissue fibrosis, intermediate immune responses, and existing functional deficits. This inquiry was performed using a porcine peroneus tertius (PT) VML model,<sup>10,15,16</sup> wherein delayed debridement of the injured muscle compartment was performed 3 months postinjury and observed for an additional month after debridement. Additionally, a second group of pigs underwent initial VML injury and were observed out to 1 month postinjury, allowing a comparative analysis of the local wound responses between initial sterile VML injury and delayed debridement. To our knowledge, all VML animal studies but one murine model<sup>17</sup> have immediately repaired the surgical tissue defect, making comparisons of acute and debrided tissue responses particularly informative to the relevance of current animal models of VML.

## METHODS

### Study design

Female Yorkshire Cross swine ( $n = 8$ ) were purchased from Midwest Research Swine (Gibbon, MN). Swine were individually housed with access to environmental enrichment, water, and daily feedings. On average, the swine were  $40.5 \pm 4.6$  kg and  $3.6 \pm 0.1$  months of age and considered to be young-adults at the time of surgery. Swine were randomized to one of three groups referred to as: the sham-operated group ( $n = 2$ , total observations of bilateral limbs  $n = 4$ ); the debridement group ( $n = 3$ ); and the acute group ( $n = 3$ ). The sham-operated group served as growth controls across the study. The debridement group underwent VML injury in the PT muscle, surgical debridement 12 weeks later, and then was observed for an additional 4 weeks out to a total of 16 weeks postinjury. The acute group also underwent PT muscle VML injury and was followed to 4 weeks postinjury. All swine underwent presurgical and postsurgical neuromuscular functional testing and computed tomography (CT) imaging. Histology and a wound healing gene expression was performed on tissues collected at the terminal time point for each group (i.e., the sham-operated group = 4 and 16; the debridement group = 16; and the acute group = 4 weeks postinjury). The study design is depicted in **Table 1**. All protocols and animal care guidelines were approved by the Institutional Animal Care and Use Committee at the United States Army Institute of Surgical Research, in compliance with the Animal Welfare Act, the Implementing Animal Welfare Regulations, and in accordance with the principles of the Guide for the Care and Use of Laboratory Animals.

**Table 1** Overview of study assessments

	Pre-VML		Post-VML, weeks		
		4	12		16
			Debridement		
			Pre	Post	
CT imaging	✓	✓	✓	✓	✓
Histology		✓	✓		✓
Function	✓	✓	✓	✓	✓
PCR array		✓			✓

CT, computed tomography; PCR, polymerase chain reaction; VML, volumetric muscle loss

### Surgical procedures

All surgical procedures were conducted while the swine were anesthetized with Telazol (4–6 mg/kg i.m.), intubated, and maintained under isoflurane anesthesia and under the appropriate aseptic conditions. Post-VML and debridement surgery analgesic administration of Buprenorphine SR (0.01 mg/kg, s.c.), Rimadyl (4.4 mg/kg, s.c.), and Excede (5.0 mg/kg, s.c.) were conducted through 1 week postsurgically. No adverse events were noted in any of the surgical groups.

As previously described,<sup>10,15,16</sup> a VML injury was surgically created by sharp removal of a  $3 \times 3$  cm<sup>2</sup> area of muscle from the middle third of the PT muscle ( $5.27 \pm 0.09$  g). Sham operated limbs were surgically exposed and the PT muscle was isolated, but no tissue was removed. In the debridement group 3 months following the initial VML injury, the muscle unit was exposed for debridement of the fibrotic deposition (**Figure 1a–d**). The original skin incision was re-incised and underlying fascia incised in line with the skin incision. The fascial layers were sharply elevated and debulked to remove adherent fascial tissue scarred to the remaining muscle. The fibrosis that filled the VML area was then sharply debrided proximally, distally, and ventrally to grossly normal muscle. Any bleeding was controlled by light pressure. In all cases, the incision was closed in the same fashion, specifically the fascia and skin were closed in layers with interrupted absorbable suture, and compressive bandages were wrapped around each limb.

### Computed tomography imaging

Standard imaging studies of the lower limbs were conducted using a Toshiba 160 slice CT and the 0.5-mm thick slices were taken prior to *in vivo* function testing presurgically, at 4, 12 (predebridement and postdebridement), and 16 weeks post-VML as appropriate. The volume of the anterior compartment was analyzed from the coronal 2D images and then reconstructed into a 3D model (Vitrea Vital Medical Imaging Software). Volume measurements were normalized to body mass.

### Neuromuscular strength testing

As previously described,<sup>10,18</sup> the strength of the dorsiflexor muscles of the anterior compartment was assessed by subdermal stimulation of the peroneal nerve using needle electrodes over a range of joint angles (0°–50°). Maximal isometric tetanic torque was elicited using 100 Hz, 0.1 ms pulse, over 800 ms (Grass S88 stimulator and 890A Aurora

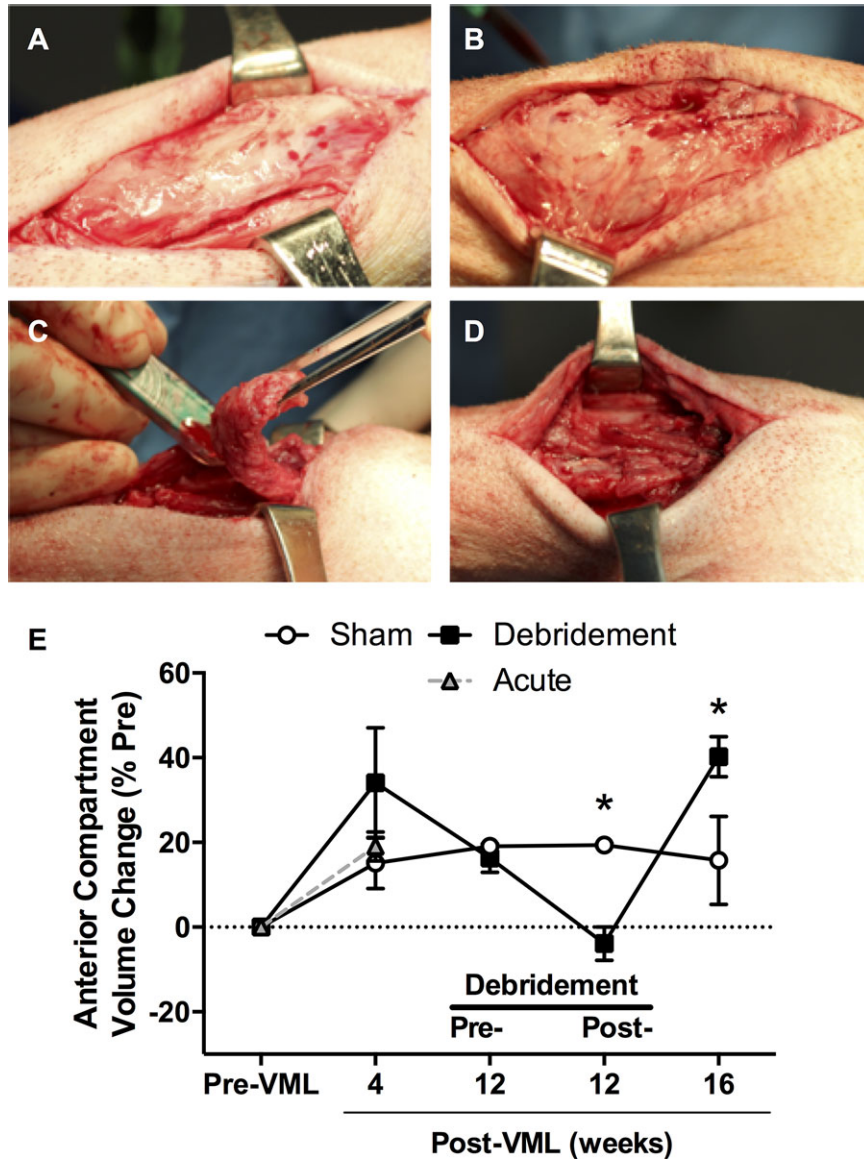


**Figure 1** Debridement induces increases in compartment volume. Peroneus tertius muscles underwent volumetric muscle loss (VML) injury. (a and b) Twelve weeks after VML injury, fibrous tissue enveloped the anterior compartment (c and d) at which time the overlaying fibrous tissue was surgically debrided. (e) Lower limb anterior compartment volume was measured using computed tomography imaging at the times specified. Values are means  $\pm$  SE; \*The debridement group;  $\neq$  the sham-operated group;  $P < 0.05$ .

Scientific). Torque was normalized to body weight assessed immediately prior to each procedure and volume of the anterior compartment.

### Histological analyses

Muscle samples from the PT muscle were excised using an 8 mm biopsy punch through the full thickness of the muscle, following the terminal functional assessment. Muscle sections were frozen in melting isopentane and stored at  $-80^{\circ}\text{C}$  until processing and analysis. Sections were processed using standard histologic procedures, with each section being cross-sectioned at  $8\ \mu\text{m}$  and stained using hematoxylin and eosin and Masson's trichrome. Additionally, portions of the fibrotic deposition overlying the PT muscle

were collected both at the time of debridement and terminally. The samples were then stored in 10% formalin for pathological processing and staining of hematoxylin and eosin and Masson's trichrome. Bright field images were acquired with a Zeiss Axio Scan.Z1 (Carl Zeiss Microscopy, Thornwood, NY) and composite images were saved separately as 24-bit, 96 dpi color images. For display purposes only, images were produced in Adobe Photoshop (Adobe Systems, San Jose, CA) by down-converting, without introducing any changes in brightness or contrast. Independent investigation of the skeletal muscle and fibrotic tissue was conducted by a board certified veterinary pathologist blinded to the experimental group. Evaluations quantified spindle cells and connective tissue matrix in the fibrotic deposition.

During all imaging and investigation, investigators were blinded to the experimental group.

### Gene expression

Biopsied tissue from the VML defect or midbelly of the PT muscle (the sham-operated group) was immediately placed in TRIzol and snap frozen in liquid nitrogen. RNA was isolated from the homogenized tissue using the TRIzol method. RNA samples were transcribed into cDNA and used for porcine-specific array analysis in the RT<sup>2</sup>Profiler polymerase chain reaction (PCR) array for wound healing (Catalog #PASS-121Z; SABiosciences, Frederick, MD) per the manufacturer's instructions. The raw fluorescence data were processed with glyceraldehyde 3-phosphate dehydrogenase serving as the endogenous controls through geometric averaging.<sup>19,20</sup> Expression ( $n = 3$  per group) of each target gene was calculated relative to samples from the sham-operated group.

### Statistical analyses

All data were analyzed using Prism 6 for Mac OSX (Graphpad, La Jolla, CA). Sample sizes of at least three per experimental group were determined prior to the study to allow for the detection of a 33% increase in muscle torque production at power (1–β) of 0.80 and  $\alpha$  of 0.05, with a shared SD of 0.025 Nm/kg. For all data, normal distribution was assumed and analysis was conducted using parametric tests. Dependent variables for CT, histology, and neuromuscular strength were analyzed separately using a variety of analyses of variance (ANOVA; one-way and two-way; group by time) and, when appropriate, Tukey HSD post-hoc analysis was performed. The  $P$  values for these dependent variables were considered statistically significant at the  $\alpha < 0.05$  level. The PCR array data were compared between designated groups using the Student's  $t$  test; the unadjusted  $P$  values are listed in **Table 2**. Notation of significance following Bonferroni correction for multiple comparisons within each gene functional group were conducted and threshold  $\alpha$  levels for each functional group are listed and noted in **Table 2**. Data are reported as mean  $\pm$  SE.

## RESULTS

Prior to the study, all animals were considered healthy and had no limb or mobility impairments. Following the initial surgery and subsequent debridement, all animals (the sham-operated group,  $n = 4$ ; the debridement group,  $n = 3$ ; and the acute group,  $n = 3$ ) recovered promptly and within 24 hours displayed normal mobility and cage activity. Additionally, no adverse events occurred for the duration of the study.

### Computed tomography

The anterior compartment underwent surgical debridement of fibrous tissue that formed along the superficial surface of the injured musculature 12 weeks postinjury (**Figure 1a–d**). Longitudinal CT imaging of the lower limb anterior muscle compartment was performed to delineate volumetric changes in response to VML and surgical debridement (**Figure 1e**). In response to VML injury, the anterior compartment tended to increase ( $P = 0.097$ ) 4 weeks postinjury but was equivalent to the sham-operated group values by

12 weeks postinjury ( $P = 0.797$ ). Immediately following debridement at 12 weeks postinjury, the anterior compartment volume was reduced by  $19.8 \pm 3.2$  mL ( $P = 0.024$ ), which corresponded with the  $18.5 \pm 2.2$  mL of tissue surgically removed, through conversion of grams to mL using a tissue density of  $1.50$  g/cm<sup>3</sup>.<sup>21</sup> Four weeks following debridement (i.e., 16 weeks postinjury), the anterior compartment volume increased significantly compared with the volume measured immediately after debridement and was significantly increased compared with the sham-operated pigs 16 weeks postinjury ( $P = 0.039$ ). The magnitude of tissue bulking observed at 4 weeks after VML injury and 4 weeks after debridement were similar ( $P = 0.525$ ).

### Histology

Qualitative histological assessment of the VML injured muscles demonstrated similar gross fibrous tissue deposition 4 weeks after VML injury and 4 weeks after debridement (**Figure 2a**). For each condition, pathologic analysis of the fibrous tissue was performed by scoring the elements of the connective tissue for maturity (**Figure 2b**). Spindle cells were quantified per high-powered field and in both the acute and debridement groups there was a similar abundance of spindle cells ( $P = 0.999$ ), which is indicative of relatively immature connective tissue. The trabecular meshwork of the connective tissue matrix was assessed on scale of maturity ( $1 \geq 75\%$  to  $4 \leq 25\%$  maturity), which indicated that in both the acute and debridement groups the fibrotic tissue covering the PT muscle was relatively immature ( $P = 0.117$ ).

### Neuromuscular strength

Repeated strength measurements were performed to assess the impact of VML injury and subsequent debridement on functional loss (**Figure 3**). VML injury resulted in a significant functional deficit compared with the sham-operated limbs across all time points assessed (**Figure 3a**; ANOVA: group  $P = 0.001$ ; time  $P = 0.700$ ; and interaction  $P = 0.655$ ). Functional deficits were similar 4 weeks after VML injury and 4 weeks after debridement (16 weeks postinjury). Similar values at 4 weeks after VML injury and 4 weeks after debridement were also observed when isometric torque was normalized to the anterior compartment volume measure with CT, an index of the functional quality of the musculature (**Figure 3b**; ANOVA: group  $P = 0.021$ ; time  $P = 0.672$ ; and interaction  $P = 0.711$ ).

### Gene expression

A wound healing PCR array was used to analyze the transcriptional muscle response to the VML injury at 4 weeks postinjury and 4 weeks after debridement of the VML-injured muscle (16 weeks postinjury; **Table 2 and Figure 4**). The transcriptional responses of 81 genes related to fibrosis and inflammation of each group was normalized to that of the sham-operated controls. Four weeks after VML injury, 68 of the 81 genes analyzed were significantly upregulated (43 of 81 genes were upregulated following multiple comparison correction; see **Table 2**), broadly indicating prolonged inflammation and production of fibrotic tissue. Four weeks after debridement of the VML-injured muscle, 45 of the 81 genes analyzed were also significantly upregulated (2 of 81 genes

**Table 2** Wound healing gene expression

Gene	Post-VML (fold change vs. sham)		P value		
	Acute 4 weeks	Debridement 16 weeks	(vs. sham) 4 weeks	16 weeks	(vs. 4 weeks) 16 weeks
Extracellular matrix components ( <i>P</i> < 0.005)					
COL1A1	42.3 ± 8.1	47.1 ± 35.1	<b>0.002</b>	0.024	0.852
COL1A2	57.6 ± 8.7	42.4 ± 31.0	<b>0.002</b>	0.027	0.430
COL3A1	46.9 ± 6.0	36.4 ± 24.8	<b>0.003</b>	0.025	0.456
COL4A3	5.2 ± 2.5	4.5 ± 1.1	0.039	0.011	0.546
COL5A2	47.8 ± 6.0	35.4 ± 23.6	<b>0.003</b>	0.025	0.401
COL5A3	8.6 ± 1.2	12.1 ± 6.6	<b>0.002</b>	0.019	0.893
COL14A1	15.5 ± 3.1	12.8 ± 7.1	0.006	0.041	0.483
DCN	8.3 ± 1.4	6.5 ± 3.6	<b>0.004</b>	0.055	0.433
EDN1	6.9 ± 1.1	6.0 ± 2.0	<b>0.003</b>	0.014	0.397
VTN	9.3 ± 2.3	6.2 ± 2.6	0.008	0.043	0.247
Remodeling enzymes ( <i>P</i> < 0.004)					
CTSK	18.0 ± 2.7	18.0 ± 13.1	0.008	0.071	0.746
F13A1	6.2 ± 1.0	5.9 ± 3.1	0.018	0.077	0.701
F3	3.7 ± 0.4	6.1 ± 2.5	0.017	0.057	0.658
MMP1	92.9 ± 23.7	406.9 ± 319.8	0.021	0.022	0.502
MMP2	42.8 ± 8.1	39.4 ± 29.8	<b>0.003</b>	0.034	0.668
MMP3	14.4 ± 1.7	23.8 ± 9.6	<b>0.002</b>	0.011	0.526
MMP7	3.6 ± 0.9	5.5 ± 1.5	0.075	0.054	0.709
MMP9	789.6 ± 555.5	183.2 ± 173.7	<b>0.004</b>	0.061	0.241
PLAT	7.9 ± 0.5	7.0 ± 3.5	<b>0.001</b>	0.029	0.538
PLAU	15.6 ± 0.7	14.5 ± 8.5	<b>0.003</b>	0.033	0.614
PLAUR	31.4 ± 5.5	19.9 ± 14.2	0.005	0.058	0.296
SERPINE1	12.7 ± 2.4	15.6 ± 10.5	<b>0.001</b>	0.039	0.941
Cellular adhesion ( <i>P</i> < 0.004)					
CDH1	30.8 ± 22.9	6.4 ± 1.7	0.028	<b>0.002</b>	0.236
ITGA2	15.6 ± 5.8	21.3 ± 13.0	0.013	0.031	0.893
ITG3	4.6 ± 0.4	5.0 ± 1.9	0.016	0.048	0.775
ITGA4	13.0 ± 1.5	10.6 ± 7.4	0.010	0.102	0.521
ITGA5	14.9 ± 1.8	10.1 ± 6.1	0.005	0.058	0.287
ITGA6	7.7 ± 0.7	6.5 ± 3.6	<b>0.002</b>	0.052	0.502
ITGAV	19.3 ± 2.2	18.3 ± 12.0	<b>0.000</b>	0.023	0.669
ITGB1	12.3 ± 1.2	11.1 ± 7.0	<b>0.002</b>	0.044	0.613
ITGB3	6.3 ± 1.2	4.3 ± 1.7	0.026	0.102	0.227
ITGB5	11.9 ± 1.5	12.2 ± 8.1	<b>0.002</b>	0.049	0.770
ITGB6	1.2 ± 0.1	2.0 ± 0.3	0.368	0.035	0.155
TNC	149.8 ± 18.6	112.5 ± 89.3	<b>0.002</b>	0.024	0.470
Cytoskeleton ( <i>P</i> < 0.013)					
ACTA2	8.9 ± 0.5	7.2 ± 4.2	<b>0.008</b>	0.078	0.453
ACTC1	4.4 ± 1.0	6.6 ± 2.4	<b>0.010</b>	<b>0.008</b>	0.757
RAC3	5.2 ± 0.3	4.8 ± 2.8	<b>0.000</b>	0.099	0.642
TAGLN	12.1 ± 2.0	12.7 ± 9.1	<b>0.008</b>	0.080	0.795
Inflammatory cytokines, chemokines, and signaling ( <i>P</i> < 0.003)					
CCL2	9.6 ± 0.6	5.7 ± 3.5	0.006	0.185	0.188
CD40LG	4.2 ± 0.7	4.9 ± 2.8	0.026	0.150	0.871
COX1	5.7 ± 0.8	3.8 ± 1.3	<b>0.003</b>	0.041	0.275
COX2	5.7 ± 1.1	5.0 ± 2.1	<b>0.002</b>	0.041	0.474
CSF2	28.3 ± 3.7	24.1 ± 13.9	<b>0.002</b>	0.015	0.502
CSF3	3.3 ± 1.1	3.6 ± 0.9	0.117	0.025	0.971
CXCL11	3.6 ± 0.6	3.6 ± 1.4	0.272	0.391	0.622
CXCL12	3.3 ± 0.3	3.3 ± 1.1	0.004	0.037	0.675
CXCL2	5.0 ± 1.2	3.5 ± 1.2	0.013	0.078	0.225

(Continued)

Table 2 Continued

Gene	Post-VML (fold change vs. sham)		P value		
	Acute	Debridement	(vs. sham)		(vs. 4 weeks)
	4 weeks	16 weeks	4 weeks	16 weeks	16 weeks
EPHB2	6.3 ± 1.1	6.1 ± 1.9	0.009	0.026	0.575
IFNG	3.7 ± 1.0	3.0 ± 1.7	0.271	0.657	0.497
IL10	10.4 ± 2.3	11.6 ± 7.9	0.013	0.074	0.855
IL1A	18.6 ± 6.5	10.0 ± 5.4	0.007	0.066	0.223
IL1B1	4.5 ± 1.3	8.3 ± 4.0	0.117	0.071	0.598
IL4	7.4 ± 2.3	8.0 ± 5.4	0.012	0.126	0.888
IL6ST	4.6 ± 0.3	4.3 ± 1.8	<b>0.000</b>	0.035	0.577
MIF	10.6 ± 1.4	7.9 ± 4.8	<b>0.001</b>	0.056	0.392
MYLK	4.8 ± 0.6	4.0 ± 1.6	0.027	0.102	0.388
STAT3	6.2 ± 0.5	5.6 ± 2.6	<b>0.000</b>	0.026	0.540
TNF	4.2 ± 1.1	3.6 ± 2.1	0.074	0.265	0.627
Growth factors and signaling ( <i>P</i> < 0.004)					
AKT1	7.1 ± 0.7	6.9 ± 4.0	<b>0.001</b>	0.050	0.684
ANGPT1	2.9 ± 0.2	3.1 ± 1.3	<b>0.004</b>	0.093	0.883
CTGF	13.2 ± 4.1	10.3 ± 6.0	<b>0.003</b>	0.036	0.482
EGF	0.7 ± 0.2	1.0 ± 0.1	0.159	0.852	0.082
EGFR	5.1 ± 0.6	5.4 ± 2.0	<b>0.001</b>	0.014	0.822
FGF2	4.9 ± 0.4	4.6 ± 2.4	0.020	0.114	0.624
FGF7	16.9 ± 0.9	16.9 ± 12.2	<b>0.002</b>	0.053	0.735
FGF10	7.1 ± 2.0	6.2 ± 2.2	0.060	0.108	0.491
HBEGF	1.5 ± 0.5	1.7 ± 0.6	0.786	0.662	0.870
IGF1	14.0 ± 1.2	15.2 ± 9.4	<b>0.001</b>	0.025	0.808
MET	3.4 ± 0.7	3.2 ± 0.9	0.006	0.014	0.560
PTEN	8.1 ± 0.5	8.6 ± 5.1	<b>0.001</b>	0.039	0.800
VEGFA	1.3 ± 0.2	2.1 ± 0.5	0.442	0.127	0.437
TGF- $\beta$ signaling ( <i>P</i> < 0.008)					
SMAD3	3.6 ± 0.4	3.6 ± 1.4	<b>0.002</b>	0.043	0.735
TGFA	5.6 ± 3.9	0.3 ± 0.1	0.171	0.022	0.251
TGF- $\beta$ 1	11.9 ± 1.0	10.8 ± 6.6	<b>0.003</b>	0.042	0.607
TGF- $\beta$ 2	8.0 ± 1.7	4.3 ± 1.5	<b>0.002</b>	0.036	0.089
TGF- $\beta$ 3	31.9 ± 5.3	25.6 ± 15.3	<b>0.002</b>	0.016	0.458
TGF- $\beta$ R3	6.5 ± 1.2	5.0 ± 2.0	<b>0.007</b>	0.042	0.327
Wnt signaling ( <i>P</i> < 0.017)					
CTNBN1	6.1 ± 0.7	5.1 ± 2.6	<b>0.001</b>	0.052	0.476
WISP1	103.9 ± 13.9	103.1 ± 84.7	<b>0.000</b>	0.021	0.758
WNT5A	4.5 ± 0.8	5.1 ± 2.1	<b>0.003</b>	0.028	0.907

VML, volumetric muscle loss.

Porcine-specific wound healing polymerase chain reaction array investigated fibrotic and inflammatory transcriptional response acutely after VML injury and delayed debridement. Gene expression fold changes are relative to the sham-operated controls.

Fold change values are means ± SE.

Bold font indicates significance following Bonferroni correction within each gene functional group,  $\alpha$  levels for each group are listed.

were upregulated following multiple comparison correction; see **Table 2**). Expression of all genes analyzed was similar between the acutely injured muscle and the injured and debrided muscle groups (**Table 2**).

## DISCUSSION

Current surgical repair of VML injuries with regenerative medicine therapies occurs after fibrous tissue has already enveloped the traumatized muscle compartment.<sup>13,14</sup> The extensive accumulation of fibrous tissue that forms acutely after VML injury is expected to interfere with neural, trophic,

vascular, and mechanical integration of regenerative implants with the remaining functional muscle fibers. Surgical debridement of overlying fibrous tissue has, therefore, been described for preparation of the VML-injured muscle to receive a regenerative medicine implant. That being said, the impact of surgical mitigation of the overlying fibrous tissue on the existing pathophysiology of VML injury is unknown, as discussed in a recent clinical report that performed surgical debridement of the VML injury prior to implantation of a regenerative medicine device.<sup>13</sup> To that end, the most salient findings of this study are: (i) that debridement 3 months after initial VML injury provoked recurrent fibrous tissue formation,

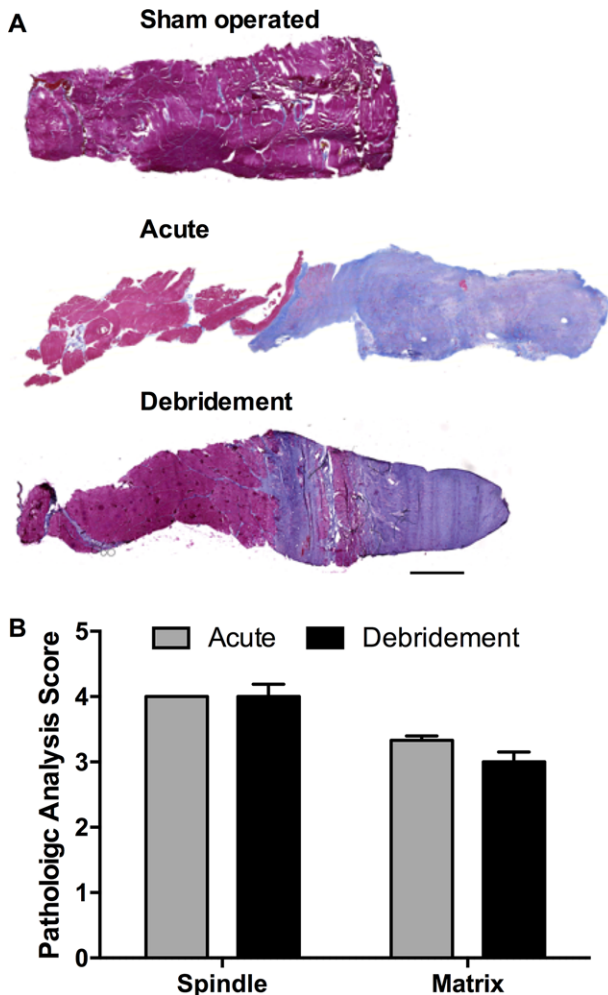


**Figure 2** Recurrent fibrosis is observed 4 weeks after debridement of volumetric muscle loss (VML) injured muscle. Histological peroneus tertius muscle sections from the sham-operated group and VML injured muscles 4 weeks after injury (the acute group) and 4 weeks after debridement were stained with Masson's Trichrome (presented in **a**) and hematoxylin and eosin (scored by veterinary pathologist in **b**). (a) Full-thickness sections from the VML defect region; red = muscle tissue, blue = fibrotic tissue. Scale bar = 2000  $\mu\text{m}$ . (b) Pathological scoring of collagen deposition for spindle cell abundance ( $1 \geq 100$  to  $4 \leq 400$  cells per field) and the trabecular meshwork of the connective tissue matrix on scale of maturity ( $1 \geq 75\%$  to  $4 \leq 25\%$  maturity) was assessed. Values are means  $\pm$  SE. No statistical differences were observed.

which seemed to still be an active process 4 weeks later, as a host of genes encoding extracellular matrix proteins, matrix remodeling enzymes, growth factors related to fibroblast proliferation, and innate and adaptive immune responses were upregulated (**Table 2**); (ii) the debridement neither exacerbated nor ameliorated isometric strength deficits (**Figure 3**). These findings indicate that surgical debridement of fibrous tissue overlaying a VML injury does not unduly worsen the functional capacity of the already weak musculature, but does upregulate inflammatory and fibrotic transcriptional pathways for at least 1 month after surgery.

The similar inflammatory and fibrogenic responses observed 4 weeks after VML injury or 4 weeks after debridement

of chronic VML-injured tissue highlights the need to consider antifibrotic therapies throughout the continuum of care. By definition, VML injury involves a traumatic loss of skeletal muscle tissue, which reduces isometric and isokinetic strength.<sup>1,11,13,14</sup> The overwhelming focus of current VML-related research has been on regenerating the lost musculature. However, existing clinical data of VML injury also exhibit significant wound heterogeneity that universally promotes fibrous tissue accretion that is accompanied by a loss of active range of motion.<sup>1,11,13,14</sup> The concerns of the overwhelming fibrogenic response following VML injury are not just related to the deposition of fibrous material and its physical restriction of joint range of motion or impedance of regenerative implant host integration, but perhaps more subtly the pathogenic damping of myogenic responses required for regeneration, repair, and maintenance of the remaining musculature. The extensive fibrous tissue deposition (**Figure 2**) and prolonged upregulation of genes associated with Wnt and transforming growth factor-beta (TGF- $\beta$ ), signaling a host of inflammatory cytokines and chemokines, and extracellular matrix-related proteins observed in either VML injury condition (**Figure 4**, **Table 2**) resembles the pathogenic response observed in Duchenne muscular dystrophy.<sup>22,23</sup> In this condition, fibrous tissue accrues within the muscle as regenerative potential declines. Notably, coordinated Wnt-TGF- $\beta$  signaling seems to induce fibrogenic activity specifically in muscle stem cells (e.g., satellite cells).<sup>24</sup> Relatedly, the pathogenic milieu in dystrophic muscle driven by TGF- $\beta$  signaling has also been shown to induce fibrogenic plasticity in multiple progenitor cells within skeletal muscle, which diminishes the regenerative capacity of the musculature that facilitates progressive muscle degeneration.<sup>25</sup> Although not empirically tested, a retrospective analysis of disability rating in VML-injured service members indicated greater disability as a function of time postinjury, suggesting progressive deterioration of limb function.<sup>2</sup> Collectively, it is clear that the fibrogenic response after VML injury can directly impair limb function and likely impedes regenerative efforts (endogenous and therapeutic), and, as such, requires therapeutic consideration.

The use of pharmacological inhibitors of fibrosis is an apparent important inclusion in the paradigm of care for VML injuries. The current data highlight numerous targets to explore, such as connective tissue growth factor (CTGF), TGF- $\beta$ , fibroblast growth factor (FGF), or Wnt5a, to attenuate the gross fibrogenic response. These targets are broadly implicated in fibrotic pathogenesis in multiple organs and tissues, including skeletal muscle, and each have currently US Food and Drug Administration approved or ongoing clinical trials to attenuate fibrosis in various conditions, such as idiopathic pulmonary fibrosis and Duchenne muscular dystrophy.<sup>26-28</sup> However, manipulating the balance between fibrogenic and myogenic responses may be complicated by shared pathways that induce competing effects. For example, overexpression of Wnt5a can induce fibroblast proliferation and extracellular matrix protein secretion leading to cardiac and presumably skeletal muscle, fibrosis<sup>29</sup>; however, Wnt5a signaling also promotes satellite cell proliferation, a key event in adult skeletal muscle regeneration.<sup>30</sup> There seem to be multiple therapeutic opportunities to

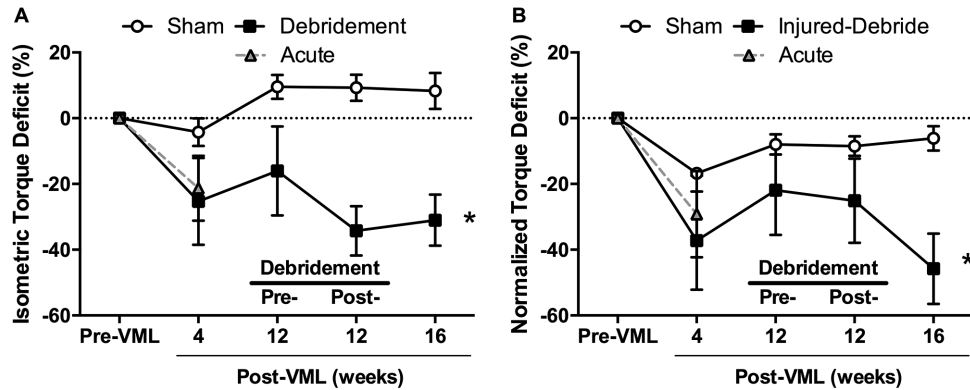


**Figure 3** Skeletal muscle strength deficits after volumetric muscle loss (VML) injury are not compounded by debridement. *In vivo* isometric torque was measured at the times specified in response to maximal peroneal nerve stimulation. (a) Absolute torque deficits and (b) torque normalized to anterior compartment volume, an index of functional quality, were calculated as a percentage of pre-VML torque. Values are means  $\pm$  SE; \*VML (acute and debridement groups); # the sham-operated group at all times postinjury;  $P < 0.05$ .

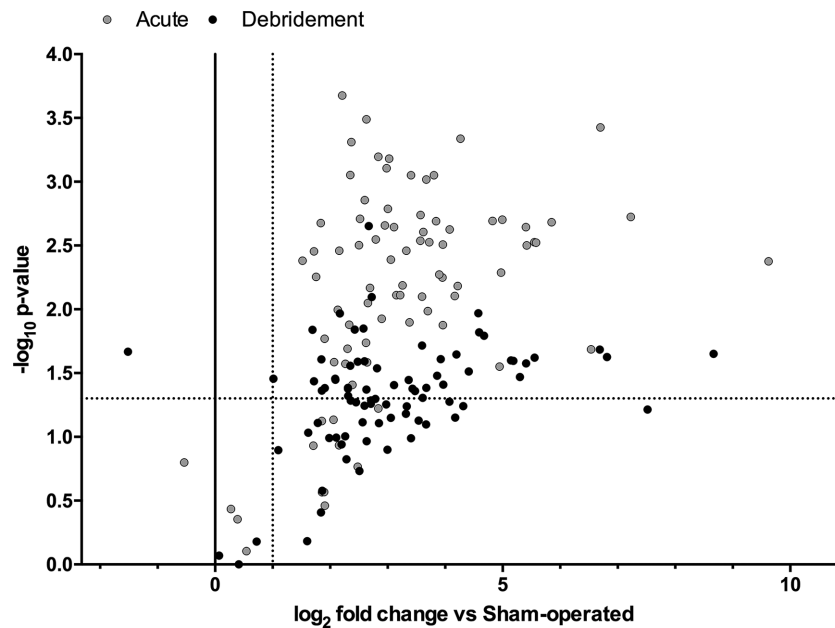


**Figure 4** Wound healing polymerase chain reaction array analysis presents upregulation of fibrotic and inflammatory transcriptional pathways after acutely after volumetric muscle loss injury and delayed debridement. Gene expression fold changes relative to the sham-operated controls and related  $P$  values are presented. The dotted horizontal and longitudinal axes indicate the lower thresholds for statistical ( $P < 0.05$ ) and biological significance (twofold change) of expression.

use antifibrotic therapies following VML injury. For example, administration acutely after injury may prevent the initial development of compartmental fibrosis and ensuing myofasciocutaneous tethering that is associated with loss of active joint range of motion following VML injury.<sup>11</sup> Adjunct administration with regenerative therapies may also be beneficial by inhibiting fibrogenic plasticity of myogenic progenitors and thereby enhancing the capacity of the host musculature to support the regenerative implant.<sup>15</sup> In particular, regenerative medicine approaches using autologous minced muscle grafts<sup>10</sup> with adjunctive antifibrotic treatments may prove beneficial in balancing the fibrotic and myogenic response and should be investigated in future studies. Given the high prevalence of debilitating muscle conditions (e.g., VML injury) among orthopedic trauma patients,<sup>1,31,32</sup> it is

intriguing to propose a predebridement and postdebridement pharmacological antifibrotic regimen in conjunction with physical rehabilitation that effectively surgically releases the functional musculature, prevents recurrent fibrosis, and thereby partially restores joint range of motion and limb function. Surgically this approach bears similarity to open quadriceps release to ameliorate post-traumatic knee stiffness due to extra-articular fibrosis,<sup>33</sup> and may represent a means to treat massive VML injuries for which regenerative medicine therapies are not yet equipped to treat.<sup>14</sup>

The discrepancy in timing of VML injury repair in human patients and animal studies questions the clinical relevance of current animal models. Specifically, clinical repair of VML injury has occurred in a delayed setting following debridement,<sup>13,14</sup> whereas all but one<sup>17</sup> animal study



has used immediate VML injury repair. Wound exudate from severely traumatized limbs presents extraordinarily high concentrations of pro-inflammatory cytokines acutely after injury and debridement,<sup>12</sup> which is likely driven by initial wound contamination as well as extensive tissue injury. Current animal VML models are sterile and, therefore, these models do not likely mirror the sheer magnitude or composition of immune responses observed clinically. That being said, VML animal models do present chronic functional deficits secondary to a permanent loss of muscle fibers,<sup>34–36</sup> which have also been shown to impair endogenously healing and rhBMP-2 mediated fracture healing,<sup>8,37,38</sup> in manner akin to type III open fracture. Therapeutic interventions that attenuate local VML-induced inflammation have also been shown to improve musculoskeletal healing,<sup>39,40</sup> indicating that the immune response elicited by sterile VML injury challenges muscle and skeletal regeneration. Notably, the current study demonstrates a similar wound healing transcriptional response and fibrous tissue formation following VML injury of pristine musculature or debridement of VML-injured musculature, indicating that surgical trauma in the absence of infection is consistent in each condition. In this regard, the current study bolsters the clinical relevance of acute sterile VML models to mimic the wound healing environment following delayed debridement of fibrosed musculature, the most likely scenario for clinical intervention.

The current study describes the wound healing response following acute VML injury and delayed debridement. In both conditions, a similar transcriptional fibrotic and inflammatory response marked by expansive fibrotic tissue accretion was observed. Molecular targets shared among conditions of fibrotic pathogenesis (e.g., CTGF, TGF- $\beta$ , FGF, and Wnt) are also implicated in VML injury. Notably, functional outcomes were not unduly worsened due to the potential removal of viable muscle fibers during debridement<sup>41</sup> or the re-ignition of exacerbated immune responses within the VML-injured tissue,<sup>8,9</sup> which are likely inhospitable to muscle regeneration.<sup>42</sup> That being said, debridement did not promote functional improvements, potentially due to rapid recurrent fibrosis. These data provide important information regarding the inclusion of antifibrotic therapies to the treatment paradigm of VML injury.

**Acknowledgments.** We gratefully acknowledge the USAISR Veterinary Support and Comparative Pathology Branches, Monica Jalomo, and Javier Chapa for technical assistance in the completion of these studies.

**Source of Funding.** Studies were funded through the Congressionally Directed Medical Research Program (Award #MR140099 awarded to B.T.C.).

**Disclaimer.** The opinions or assertions contained herein are the private views of the authors and are not to be construed as official or as reflecting the views of the Department of the Army, the Department of Defense, or the United States Government.

**Author Contributions.** B.T.C. and S.M.G. wrote the manuscript. B.T.C. and S.M.G. designed the research. B.T.C., J.C.R., and S.M.G. performed the research. B.T.C. and S.M.G. analyzed the data.

**Conflict of Interest.** The authors declared no conflict of interest.

1. Corona, B.T., Rivera, J.C., Owens, J.G., Wenke, J.C. & Rathbone, C.R. Volumetric muscle loss leads to permanent disability following extremity trauma. *J. Rehabil. Res. Dev.* **52**, 785–792 (2015).
2. Rivera, J.C. & Corona, B.T. Muscle-related disability following combat injury increases with time. *US Army Med. Dep. J.* 30–34 (2016).
3. Corona, B.T., Wenke, J.C. & Ward, C.L. Pathophysiology of volumetric muscle loss injury. *Cells Tissues Organs* **202**, 180–188 (2016).
4. Stratos, I., Graff, J., Rotter, R., Mittlmeier, T. & Vollmar, B. Open blunt crush injury of different severity determines nature and extent of local tissue regeneration and repair. *J. Orthop. Res.* **28**, 950–957 (2010).
5. Criswell, T.L. et al. Compression-induced muscle injury in rats that mimics compartment syndrome in humans. *Am. J. Pathol.* **180**, 787–797 (2012).
6. Ingalls, C.P., Warren, G.L. & Armstrong, R.B. Dissociation of force production from MHC and actin contents in muscles injured by eccentric contractions. *J. Muscle Res. Cell Motil.* **19**, 215–224 (1998).
7. Warren, G.L. et al. Chemokine receptor CCR2 involvement in skeletal muscle regeneration. *FASEB J.* **19**, 413–415 (2005).
8. Hurtgen, B.J. et al. Severe muscle trauma triggers heightened and prolonged local musculoskeletal inflammation and impairs adjacent tibia fracture healing. *J. Musculoskelet. Neuronal Interact.* **16**, 122–134 (2016).
9. Sadtler, K. et al. Developing a pro-regenerative biomaterial scaffold microenvironment requires T helper 2 cells. *Science* **352**, 366–370 (2016).
10. Ward, C.L., Pollot, B.E., Goldman, S.M., Greising, S.M., Wenke, J.C. & Corona, B.T. Autologous minced muscle grafts improve muscle strength in a porcine model of volumetric muscle loss injury. *J. Orthop. Trauma* **30**, e396–e403 (2016).
11. Garg, K. et al. Volumetric muscle loss: persistent functional deficits beyond frank loss of tissue. *J. Orthop. Res.* **33**, 40–46 (2015).
12. Davis, T.A., O'Brien, F.P., Anam, K., Grijalva, S., Potter, B.K., & Elster, E.A. Heterotopic ossification in complex orthopaedic combat wounds: quantification and characterization of osteogenic precursor cell activity in traumatized muscle. *J. Bone Joint Surg. Am.* **93**, 1122–1131 (2011).
13. Dziki, J. et al. An acellular biologic scaffold treatment for volumetric muscle loss: results of a 13-patient cohort study. *NPJ Regen. Med.* **1**, 16008 (2016).
14. Mase, V.J. Jr et al. Clinical application of an acellular biologic scaffold for surgical repair of a large, traumatic quadriceps femoris muscle defect. *Orthopedics* **33**, 511 (2010).
15. Corona, B.T. & Greising, S.M. Challenges to acellular biological scaffold mediated skeletal muscle tissue regeneration. *Biomaterials* **104**, 238–246 (2016).
16. Pollot, B.E. & Corona, B.T. Volumetric muscle loss. *Methods Mol. Biol.* **1460**, 19–31 (2016).
17. Quarta, M. et al. Bioengineered constructs combined with exercise enhance stem cell-mediated treatment of volumetric muscle loss. *Nat. Commun.* **8**, 15613 (2017).
18. Kheirabadi, B.S. et al. Long-term effects of Combat Ready Clamp application to control junctional hemorrhage in swine. *J. Trauma Acute Care Surg.* **77** (3 Suppl 2), S101–S108 (2014).
19. Vandesompele, J. et al. Accurate normalization of real-time quantitative RT-PCR data by geometric averaging of multiple internal control genes. *Genome Biol.* **3**, RESEARCH0034 (2002).
20. Ruijter, J.M. et al. Amplification efficiency: linking baseline and bias in the analysis of quantitative PCR data. *Nucleic Acids Res.* **37**, e45 (2009).
21. Swann, D.A., Garg, H.G., Jung, W. & Hermann, H. Studies on human scar tissue proteoglycans. *J. Invest. Dermatol.* **84**, 527–531 (1985).
22. Smith, L.R., Hammers, D.W., Sweeney, H.L. & Barton, E.R. Increased collagen cross-linking is a signature of dystrophin-deficient muscle. *Muscle Nerve* **54**, 71–78 (2016).
23. Song, Y. et al. Expression levels of TGF- $\beta$ 1 and CTGF are associated with the severity of Duchenne muscular dystrophy. *Exp. Ther. Med.* **13**, 1209–1214 (2017).
24. Biressi, S., Miyabara, E.H., Gopinath, S.D., Carlig, P.M. & Rando, T.A. A Wnt-TGF $\beta$ 2 axis induces a fibrogenic program in muscle stem cells from dystrophic mice. *Sci. Transl. Med.* **6**, 267ra176 (2014).
25. Pessina, P. et al. Fibrogenic cell plasticity blunts tissue regeneration and aggravates muscular dystrophy. *Stem Cell Reports* **4**, 1046–1060 (2015).
26. Lehtonen, S.T. et al. Pirfenidone and nintedanib modulate properties of fibroblasts and myofibroblasts in idiopathic pulmonary fibrosis. *Respir. Res.* **17**, 14 (2016).
27. Morales, M.G. et al. Reducing CTGF/CNN2 slows down mdx muscle dystrophy and improves cell therapy. *Hum. Mol. Genet.* **22**, 4938–4951 (2013).
28. Wollin, L., Maillet, I., Quesniaux, V., Holweg, A. & Ryffel, B. Antifibrotic and anti-inflammatory activity of the tyrosine kinase inhibitor nintedanib in experimental models of lung fibrosis. *J. Pharmacol. Exp. Ther.* **349**, 209–220 (2014).
29. Newman, D.R. et al. Expression of WNT5A in idiopathic pulmonary fibrosis and its control by TGF- $\beta$  and WNT7B in human lung fibroblasts. *J. Histochem. Cytochem.* **64**, 99–111 (2016).

30. Otto, A. *et al.* Canonical Wnt signalling induces satellite-cell proliferation during adult skeletal muscle regeneration. *J. Cell Sci.* **121** (Pt 17), 2939–2950 (2008).
31. MacKenzie, E.J. *et al.* Long-term persistence of disability following severe lower-limb trauma. Results of a seven-year follow-up. *J. Bone Joint Surg. Am.* **87**, 1801–1809 (2005).
32. Cross, J.D., Ficke, J.R., Hsu, J.R., Masini, B.D. & Wenke, J.C. Battlefield orthopaedic injuries cause the majority of long-term disabilities. *J. Am. Acad. Orthop. Surg.* **19** Suppl 1, S1–S7 (2011).
33. Pujol, N., Boisrenoult, P. & Beaufils, P. Post-traumatic knee stiffness: surgical techniques. *Orthop. Traumatol. Surg. Res.* **101**, (1 Suppl) S179–S186 (2015).
34. Aurora, A., Garg, K., Corona, B.T. & Walters, T.J. Physical rehabilitation improves muscle function following volumetric muscle loss injury. *BMC Sports Sci. Med. Rehabil.* **6**, 41 (2014).
35. Aurora, A., Roe, J.L., Corona, B.T. & Walters, T.J. An acellular biologic scaffold does not regenerate appreciable de novo muscle tissue in rat models of volumetric muscle loss injury. *Biomaterials* **67**, 393–407 (2015).
36. Ward, C.L., Ji, L. & Corona, B.T. An autologous muscle tissue expansion approach for the treatment of volumetric muscle loss. *Biores. Open Access* **4**, 198–208 (2015).
37. Pollot, B.E., Goldman, S.M., Wenke, J.C. & Corona, B.T. Decellularized extracellular matrix repair of volumetric muscle loss injury impairs adjacent bone healing in a rat model of complex musculoskeletal trauma. *J. Trauma Acute Care Surg.* **81** (8 Suppl 2 Proceedings of the 2015 Military Health System Research Symposium), S184–S190 (2016).
38. Willett, N.J. *et al.* Attenuated human bone morphogenetic protein-2-mediated bone regeneration in a rat model of composite bone and muscle injury. *Tissue Eng. Part C Methods* **19**, 316–325 (2013).
39. Hurtgen, B.J. *et al.* Impairment of early fracture healing by skeletal muscle trauma is restored by FK506. *BMC Musculoskelet. Disord.* **18**, 253 (2017).
40. Hurtgen, B.J. *et al.* Autologous minced muscle grafts improve endogenous fracture healing and muscle strength after musculoskeletal trauma. *Physiol. Rep.* **5**, e13362 (2017).
41. Sassooun, A. *et al.* Muscle viability revisited: are we removing normal muscle? A critical evaluation of dogmatic debridement. *J. Orthop. Trauma* **30**, 17–21 (2016).
42. Tidball, J.G. & Villalta, S.A. Regulatory interactions between muscle and the immune system during muscle regeneration. *Am. J. Physiol. Regul. Integr. Comp. Physiol.* **298**, R1173–R1187 (2010).

© 2017 The Authors. Clinical and Translational Science published by Wiley Periodicals, Inc. on behalf of American Society for Clinical Pharmacology and Therapeutics. This is an open access article under the terms of the Creative Commons Attribution-NonCommercial License, which permits use, distribution and reproduction in any medium, provided the original work is properly cited and is not used for commercial purposes.